Behavior of Vertical Boundary Elements in Steel Plate Shear Walls

BING QU and MICHEL BRUNEAU

ABSTRACT

The AISC *Seismic Provisions* and CSA S-16 Standard require a minimum moment of inertia for the vertical boundary elements (VBEs) in steel plate shear walls (SPSWs) to avoid undesirable VBE behaviors. The equation limiting VBE flexibility has been derived from a flexibility factor, ω_t, developed in plate girder theory and the limit on VBE flexibility has been empirically specified based on previous test results. This paper reviews the derivations of the flexibility factor and how that factor was incorporated into current code design requirements for SPSWs. Then, analytical models to prevent VBE shear yielding and to estimate the out-of-plane buckling strength of VBE are developed, followed by a review of past experimental data to investigate if the significant inward VBE inelastic deformation and out-of-plane buckling observed in some instances were due to excessive VBE flexibilities or other causes such as shear yielding at the ends of the VBEs. It is shown that the existing limit on ω_t is uncorrelated to satisfactory in-plane and out-of-plane VBE performance. The proposed analytical models predict performance of previously tested SPSWs that correlates well with the experimental observations.

Keywords: steel plate shear walls, vertical boundary elements, shear yielding, out-of-plane buckling.

A typical steel plate shear wall (SPSW) such as the one shown in Figure 1 consists of infill steel panels surrounded by columns, called vertical boundary elements (VBEs), on each side, and beams, called horizontal boundary elements (HBEs), above and below. These infill panels are allowed to buckle in shear and subsequently form diagonal tension fields when resisting lateral loads. Energy dissipation of SPSW during seismic events is principally achieved through yielding of the panels along the diagonal tension fields (Sabelli and Bruneau, 2007). Consistent with capacity design principles, the Canadian Standard S16 on *Limit States Design of Steel Structures* (CSA, 2001) and the AISC *Seismic Provisions for Structural Steel Buildings* (AISC, 2005c) require HBEs and VBEs to be designed to remain elastic when the infill panels are fully yielded, with the exception of plastic hinges at the ends of HBEs and at the VBE bases that are needed to develop the expected plastic mechanism of the wall when rigid HBE-to-VBE and VBE-to-ground connections are used. The procedures to achieve capacity design of the boundary frame of SPSWs have been presented by Berman and Bruneau (2008), Vian and Bruneau (2005),

Qu and Bruneau (2008). Using the knowledge on capacity design, as well as building on findings from a recent study of HBEs that provided new insights on the design demands and capacities to consider for their design (Qu and Bruneau, 2008), a study was undertaken to reassess demands on VBEs, and the relevance in that context of existing provisions that limit VBE flexibility.

The early Canadian provisions for SPSWs (i.e., CSA Standard S16-94 [CSA, 1994]) required VBEs to be designed as beam-column using a conventional strength-based approach. This approach was challenged by the results of tests on quarter-scale SPSW specimens by Lubell et. al (2000), in which the VBEs designed using the strength-based approach
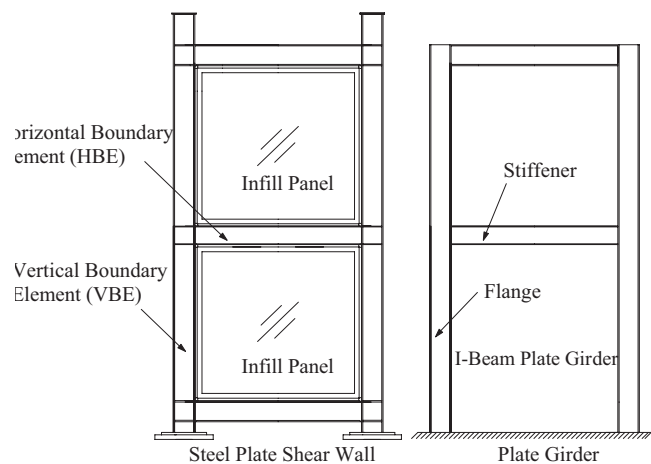
Bing Qu, Ph.D., Assistant Professor, Department of Civil and Environmental Engineering, California Polytechnic State University, One Grand Ave., San Luis Obispo, CA 93407 (corresponding author). E-mail: bqu@calpoly.edu

Michel Bruneau, Ph.D., P.Eng., Professor, Department of Civil, Structural and Environmental Engineering, University at Buffalo, 130 Ketter Hall, Buffalo, NY 14260. E-mail: bruneau@buffalo.edu

Fig. 1. Typical steel plate shear wall and analogous vertical cantilever plate girder.

exhibited significant "pull-in" deformation or undesirable premature out-of-plane buckling. In a subsequent discussion of the Lubell et al. SPSW specimens, Montgomery and Medhekar (2001) attributed this poor performance to insufficient VBE stiffness, and that rationale was accepted in the development of CSA-S16 provisions. If VBEs deform excessively, they may be unable to anchor the infill panel yield forces. A non-uniform diagonal tension field may then develop and affect the VBEs inconsistently to the design assumptions.

To ensure adequately stiff VBEs, CSA S16-01 (CSA, 2001) introduced the flexibility factor, ω_t, proposed in previous analytical work of plate girder theory, as an index of VBE flexibility. Please note that this flexibility factor, ω_t, is different from the other symbol, ω, which is used in the later sections of this paper for denoting the distributed infill panel forces. Noting that the Lubell et al. specimens had flexibility factors of 3.35, and that all other known tested SPSWs that behaved in a ductile manner had flexibility factors of 2.5 or less, CSA S16-01 empirically specified an upper bound of 2.5 on ω_t. Note that this requirement can be converted into the VBE flexibility requirement presented in the current design codes as demonstrated later.

In design, the intent is that the aforementioned flexibility limit prevents excessively slender VBE. However, beyond the empirical observations and analogy to plate girder theory, no work has investigated whether the significant inward inelastic deformations of VBEs observed in past tests were directly caused by excessive VBE flexibilities or due to other causes, such as shear yielding at the ends of VBEs. In addition, no theoretical research has established a relationship between ω_t and the out-of-plane buckling strength of VBE as part of SPSW behavior.

To better understand the preceeding issues, in this paper, derivation of the flexibility factor in plate girder theory is first reviewed, followed by the description of how that factor was incorporated into the current design codes. Then, analytical models for preventing VBE shear yielding and for estimating the out-of-plane buckling strength of VBEs are developed. Finally, results from some previously tested SPSWs are revisited and assessed to validate the proposed analytical models.

REVIEW OF FLEXIBILITY FACTOR IN PLATE GIRDER THEORY

In the SPSW literature, SPSWs are often described like cantilever vertical plate girders. Using this analogy, the story height and bay width of a SPSW are analogous to the stiffener spacing and the depth of a plate girder, respectively, as shown in Figure 1. Note that this analogy has only qualitative merits in providing a conceptual understanding of the VBE behavior in a SPSW. Berman and Bruneau (2004) have identified that many significant differences exist in the strengths and behavior of these two systems.

Nonetheless, plate girder studies provided the theoretical framework from which Equation 1 that will be introduced in detail later was originally derived. The CSA S16-01 and the AISC *Seismic Provisions* reference Wagner's analytical studies (Wagner, 1931) on the elastic behavior of girders with thin metal webs subjected to transverse shear, where a method for determining the minimum moments of inertia of flanges to ensure a sufficiently uniform tension field across the web plate has been developed. Since that method is the one underlying the current flexibility limit for VBE design, a brief review of that study is presented here. The symbols used in the original work have been changed to fit the nomenclatures used for SPSW design.

Wagner's analysis postulated that the deformation of a cantilever plate girder of elastic behavior under transverse load can be schematically shown as in Figure 2. The subscripts o and u are assigned to the variables corresponding to the top and bottom flanges, respectively. As shown in Figure 2, plate girder flange deformation is obtained by superposing two effects, namely, global deflection of the plate girder due to transverse load, represented by δ, and local deflections of the flanges between neighboring stiffeners due to elastic web tension actions, represented by η_u and η_o. In Figure 2, L is the depth of the plate girder; and α is the inclination of infill tension actions.

Uniformity of the tension field across the web plate of the girder depends on the flexibility of flanges. To better understand this, consider the effect of a single tension diagonal, which is denoted by line "uo" in Figure 2. When the flanges are flexible and develop inward deflections (i.e., η_u and η_o shown in Figure 2) due to the web plate forces, the elongation of uo decreases, compared to the case when rigid flanges would be present, as a result of deformation compatibility. Note that this effect varies along the flanges (i.e., the elongations of tension diagonals at different locations are different), resulting in uneven tension fields across the web plate.
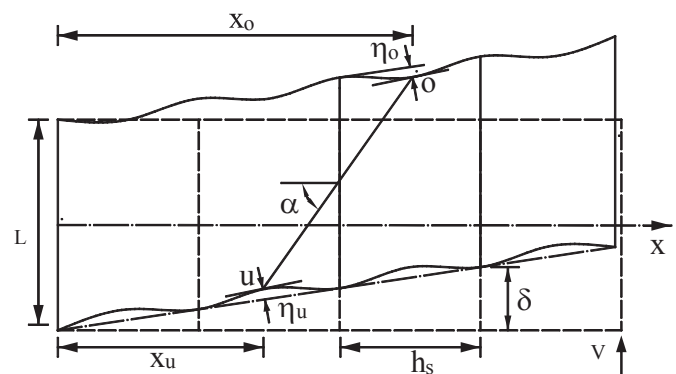

Fig. 2. Deformation of a cantilever plate girder under transverse load (adapted from Wagner, 1931).

For flanges infinitely rigid in bending, there would be no local deflections of flanges between neighbouring stiffeners, resulting in a uniform tension field across the web plate.

Modeling each flange of the plate girder as a continuous beam on elastic foundations, and accounting for the real load distribution along each flange, which can be determined by superposing the uniform load obtained assuming that the flanges are infinitely rigid and the loss of this uniform load due to flange flexibility, Wagner (1931) derived the following governing equation for the local flange deflections:

$$
\frac{d^4(\eta_u - \eta_o)}{dx^4} = \left(\frac{1}{I_u} + \frac{1}{I_o}\right) t_{wi} \sin^2 \alpha \varepsilon_g
$$
$$
- \left(\frac{1}{I_u} + \frac{1}{I_o}\right) \frac{t_{wi} \sin^4 \alpha}{L} (\eta_u - \eta_o) \tag{1}
$$

where
η_u = deflection of the bottom flange due to web tension actions
η_o = deflection of the top flange due to web tension actions
I_u = moment of inertia of the bottom flange
I_o = moment of inertia of the top flange
α = inclination angle of the web plate tension action
t_{wi} = web plate thickness
L = depth of the plate girder which corresponds by analogy to the width of a SPSW
ε_g = strain in the tension diagonals assuming that the flanges are rigid

Equation 1 is a fourth-order ordinary differential equation and can be solved for $(\eta_u - \eta_o)$ using classic procedures. The maximum value of $(\eta_u - \eta_o)$, which corresponds to the maximum loss of the of tension diagonal elastic elongation (i.e., an index of the maximum loss of the elastic uniform load along the flanges), is:

$$
(\eta_u - \eta_o)_{max} = \tag{2}
$$

$$
\frac{\varepsilon_g L}{\sin^2 \alpha} \left(1 - \frac{\sin\left(\frac{\omega_t}{2}\right)\cosh\left(\frac{\omega_t}{2}\right) + \cos\left(\frac{\omega_t}{2}\right)\sinh\left(\frac{\omega_t}{2}\right)}{\sin\left(\frac{\omega_t}{2}\right)\cos\left(\frac{\omega_t}{2}\right) + \sinh\left(\frac{\omega_t}{2}\right)\cosh\left(\frac{\omega_t}{2}\right)} \right)
$$

where
ω_t = flexibility factor, defined as:

$$
\omega_t = h_{si} \sin \alpha \sqrt[4]{\left(\frac{1}{I_u} + \frac{1}{I_o}\right)\frac{t_{wi}}{4L}} \tag{3}
$$

where
h_{si} = spacing between neighboring stiffeners in a plate girder (which corresponds by analogy to story height of a SPSW).

As explicitly expressed in Equation 3, increasing the flange stiffness of a plate girder (i.e., increasing I_u and I_o) would decrease the corresponding flexibility factor for given values of the other terms.

To assess the uniformity of the web tension field, a stress uniformity ratio, $\sigma_{mean}/\sigma_{max}$, was proposed and calculated as:

$$
\frac{\sigma_{mean}}{\sigma_{max}} = \left(\frac{2}{\omega_t}\right)\left[\frac{\cosh(\omega_t) - \cos(\omega_t)}{\sinh(\omega_t) + \sin(\omega_t)}\right] \tag{4}
$$

where
σ_{mean} = mean of the web tension force components parallel with the stiffener
σ_{max} = maximum of the web tension force components parallel with the stiffener

The relationship between the stress uniformity ratio (i.e., $\sigma_{mean}/\sigma_{max}$) and the flexibility factor (i.e., ω_t) is shown in Figure 3. As shown on that curve, for smaller values of ω_t (e.g., in the range $0 \le \omega_t \le 1$), for which the plate girder has relatively stiff flanges, the stress uniformity ratio approximately equals 1 (which physically means that the maximum stress is close to the average stress), indicating development of a uniform web tension field. However, with increases in the flexibility factor, the stress uniformity ratio decreases, indicating formation of a less uniform web tension field in plate girders having more flexible flanges.
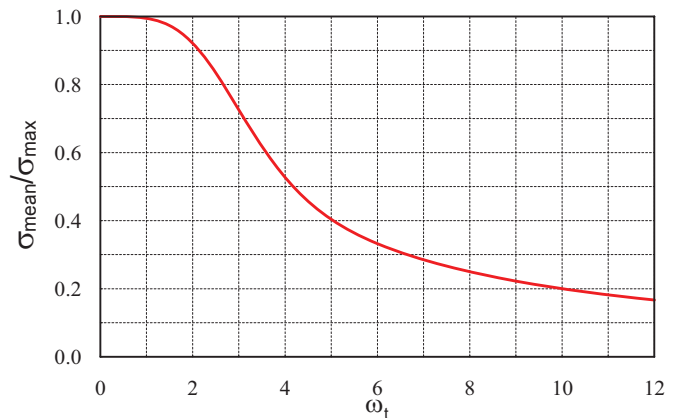

Fig. 3. Relationship between flexibility factor and stress uniformity ratio.

For simplicity, Kuhn, Peterson and Levin (1952) simplified Equation 3, by assuming $\alpha = 45°$, for which $\sin \alpha = 0.7$, and by substituting the approximate equivalency $\left(\dfrac{1}{I_u} + \dfrac{1}{I_o}\right) = \dfrac{4}{\left(I_u + I_o\right)}$, to obtain:

$$\omega_t \approx 0.7 h_s \sqrt[4]{\frac{t_{wi}}{\left(I_u + I_o\right)L}} \qquad (5)$$

Kuhn et al. (1952) proposed the stress amplification factor, C_2, which can be determined from the following equation, to characterize the uniformity of elastic web tension field:

$$\sigma_{max} = (1 + C_2)\sigma_{mean} \qquad (6)$$

As expressed in Equation 6, the stress amplification factor, C_2, captures the difference between σ_{max} and σ_{mean}. Large value of C_2 corresponds to a significant difference between σ_{max} and σ_{mean}, indicating the formation of a less uniform web tension field. Solving for C_2 with respect to the stress uniformity ratio (i.e., $\sigma_{mean}/\sigma_{max}$) from Equation 6 and recalling Equation 4, the relationship between C_2 and ω_t can be obtained and is illustrated in Figure 4. Consistent with Figure 3, the curve shown in Figure 4 indicates that a less uniform tension field (which corresponds to greater C_2) will develop in a plate girder with more flexible flanges (which corresponds to greater ω_t).

FLEXIBILITY LIMIT FOR VBE DESIGN

To quantify the minimum flexural stiffness of VBE needed to ensure uniformity of elastic infill tension fields in SPSWs and avoid the undesirable VBE behaviors described previously, CSA S16-01 adopted Equation 5. Provided that each VBE has the same moment of inertia, I_c, as normally the case in SPSWs, Equation 5 becomes:

$$\omega_t = 0.7 h_{si} \sqrt[4]{\frac{t_{wi}}{2 I_c L}} \qquad (7)$$

For the reasons described earlier, and on the strength of the information provided by Montgomery and Medhekar (2001), the CSA S16 limited this factor to a maximum value of 2.5. This limit of 2.5 was also selected on the assumption that tension fields should be sufficiently uniform for ductile behavior to develop. In Figure 4, limiting the flexibility factor to a value of 2.5 is shown to correspond to a maximum stress not exceeding by more than 20% the average stress of the web tension field. Imposing the upper bound of 2.5 on Equation 7 and solving for I_c leads to the following requirement, first implemented in the CSA S16-01:

$$I_c \geq \frac{0.00307 t_{wi} h_{si}^{4}}{L} \qquad (8)$$

The requirement was subsequently adopted in the National Earthquake Hazards Reduction Program (NEHRP) *Provisions for Seismic Regulations for New Buildings and Other Structures,* also known as FEMA 450 (FEMA, 2003), and then the AISC *Seismic Provisions* (AISC, 2005c).

Note that the analytical work by Wagner (1931) and Kuhn et al. (1952) for plate girders, which was used for determination of the VBE flexibility limit, assumed elastic behavior. Although at the onset of the tension field action, the maximum stress in an infill panel may be significantly greater than the average due to VBE deflections, this difference could decrease upon greater story drifts, provided that the boundary frame members are able to allow infill panel stress redistribution after the first yielding of tension diagonals. To better understand this, stress distributions across the first-story web plates (i.e., along the direction perpendicular to the tension diagonals) are shown in Figure 5 for two tested specimens, namely, the specimen tested by Driver et al. (1998) and the specimen tested by Lee and Tsai (2008). Note that these two specimens have different flexibility factors and will be introduced in more detail in a later section. Figure 5 shows that, as drift levels progressively increase, both specimens will ultimately develop uniform tension fields, although the specimen tested by Lee and Tsai (which had more flexible VBEs) develops less uniform tension fields at lower drift levels. Since identical uniform stress distribution ultimately develop in the panels of SPSW, the issue of initial stress distribution seems irrelevant to the performance of SPSW. By inference, this raises questions about the relevance of considering a flexibility factor altogether, ω_t, in SPSW design. Therefore, different models are investigated in the next sections to rationalize desirable and undesirable VBE behaviors.
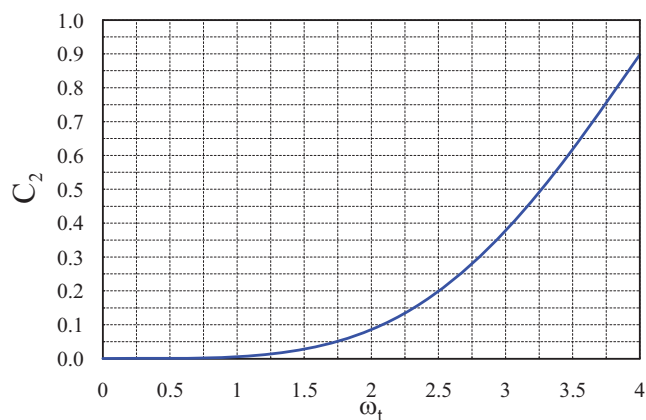
Fig. 4. Relationship between flexibility factor and stress amplification factor.

PREVENTION OF VBE IN-PLANE SHEAR YIELDING

As mentioned earlier, the significant "pull-in" deformation of VBE observed during the tests on single-story SPSWs by Lubell et al. (2000) as shown in Figure 6 was a milestone event that led to the current limit specified for the flexibility of VBEs in SPSWs (AISC, 2005c; CSA, 2001). This undesirable performance was ascribed to the insufficient VBE stiffness (Montgomery and Medhekar, 2001). However, VBE shear yielding is another important factor that may result in significant inelastic VBE deflections. At the time of this writing, no literature has reported or checked whether the previously tested specimens have encountered VBE shear yielding.

To have a better understanding of the observed significant inward deformations in VBEs, an analytical model for estimating VBE shear demand is proposed in this section followed by assessment on the previously tested SPSWs using the proposed analytical model. For comparison purpose, results from pushover analysis on strip models of those considered SPSWs are also provided. Predictions are compared with the observed behavior.
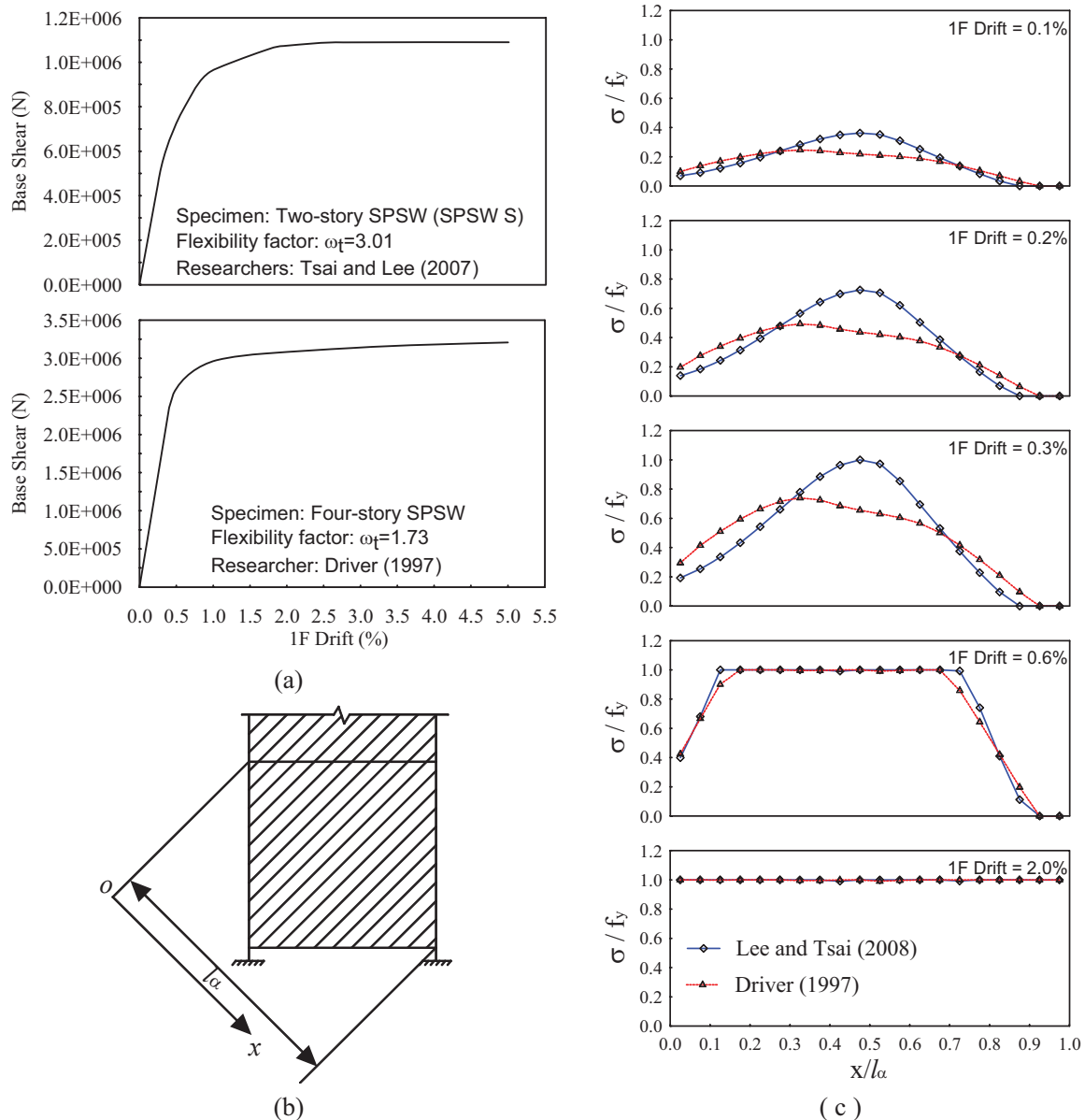

Fig. 5. Uniformity of tension fields: (a) pushover curves; (b) schematic of tension fields; (c) uniformity of panel stresses in strip models.

SHEAR DEMAND AND STRENGTH OF VBE

According to the current design codes, VBEs of a SPSW, which are sized as beam-column members (i.e., considering the P-M interaction demands), are required to remain elastic when the webs are fully yielded, with exception of plastic hinges at the VBE bases when VBEs are fixed to ground. Although not explicitly stated, those plastic hinges should be flexural-plastic hinges (i.e., as opposed to shear-yielding hinges) for the infill panels to be effectively anchored and consequently allow development of the expected tension fields. Note that the shear demands in VBEs can be of significant magnitude. One major contribution to the shear demands is due to yielding of the infill plate (incidentally this contribution produces equal and opposite shears in the opposing VBEs and thus do not contribute to the total story shear resisted). The free-body diagram of Figure 9 (explained later in this paper) for which equilibrium is explained in Berman and Bruneau (2008) is typically used to calculate these shear forces. When the resulting VBE shear demands are greater than their shear strengths, VBEs exhibit undesirable shear yielding behavior resulting in the significant pull-in deformation in VBEs as observed in some prior experimental research.

As shown in Figure 7, the free body diagram of the right-hand-side VBE at the ith story in a uniformly yielded single-bay SPSW under rightward lateral forces is used to determine the maximum VBE shear demand here. Note that the same VBE design shear force can be obtained for left-hand-side VBE based on the procedure presented later. Conservatively, assuming that the moments applied at the top and bottom ends of the VBE are equal to their expected nominal plastic moments, one can obtain the following estimate of VBE shear demand from equilibrium:

$$V_{u-design} = \frac{2R_y f_y Z_c}{h_{si}} + \frac{\omega_{xci} h_{si}}{2} + \frac{\omega_{yci} d_{ci}}{2} \qquad (9)$$
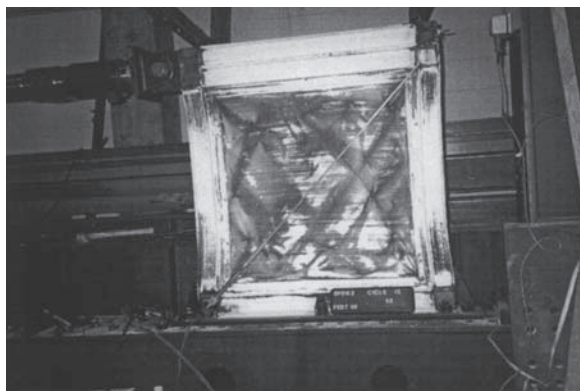
where

d_{ci}	=	VBE depth
Z_c	=	plastic section modulus of VBE
ω_{xci}	=	horizontal component of infill panel yield forces along VBE
ω_{yci}	=	vertical component of infill panel yield forces along VBE
f_y	=	yield stress of boundary frame
R_y	=	ratio of expected to nominal yield stress

Note that equations for calculating ω_{xci}, and ω_{yci} are available in Berman and Bruneau (2008).

It is recognized that Equation 9 overestimates the VBE shear design force for two reasons: (1) the plastic moments at the VBE ends may be reduced due to the presence of axial force, shear force and vertical stresses in the VBE (i.e., similar to the reduction of HBE plastic moments presented in Qu and Bruneau 2008); and (2) plastic hinges in properly designed SPSWs may develop in the HBEs, not in the VBEs. Note that for this case, the plastic moment of HBE may not necessarily distribute equally (½ and ½) between the columns above and below the connection due to higher mode effects. For expediency, it is conservative to design the columns to resist the shear force given by Equation 9, and acting concurrently with the corresponding axial force and moment. However, the true shear demand on columns may be less than given by Equation 9, and predicting the adequacy existing in SPSW VBEs using this procedure may incorrectly predict failure due to shear yielding (as will be the case for some tested SPSWs discussed in the following section).

In design, the shear demand obtained from Equation 9 should be compared to the VBE shear strength, V_n, which, when the VBE web is compact (i.e., when $h_{wci}/t_{wci} \leq 2.24\sqrt{E/f_y}$ per ANSI/AISC 360-05), is calculated as:
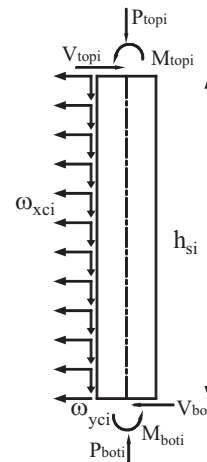

Fig. 6. Deformation and yield patterns of SPSW2 after $6\delta_y$ (Lubell et al., 2000).

Fig. 7. In-plane free body diagram of the VBE at the ith story for determination of shear demand.

Case	Researcher	Specimen Identification	Number of Stories	Scale	Aspect Ratio[c] (L/h)	α (°)	ω_t	V_n (kN)	$V_{pushover}$ (kN)	$V_{u\text{-}design}$ (kN)	Shear Yielding
(i) single-story specimen											
1	Lubell et al. (2000)	SPSW2	1	1:4	1.00	37.4	3.35	75	108	113	Yes
2	Berman and Bruneau (2005)	F2	1	1:2	2.00	44.8	1.01	932	259	261[d]	No
(ii) multi-story specimen[a]											
3	Driver et al. (1998)	[b]	4	1:2	1.58	43.4	1.73	766	1361	1458	Yes
4	Park et al. (2007)	SC2T	3	1:3	1.46	44.4	1.24	999	676	1064	No
5		SC4T	3	1:3	1.46	44.1	1.44	999	984	1383	No
6		SC6T	3	1:3	1.46	43.9	1.58	999	1218	1622	Yes
7		WC4T	3	1:3	1.46	45.0	1.62	560	920	1210	Yes
8		WC6T	3	1:3	1.46	45.0	1.77	560	1151	1461	Yes
9	Qu et al. (2008)	[b]	2	1:1	1.00	41.3	1.95	2881	1591	2341	No
10	Lee and Tsai (2007)	SPSW N	2	1:1	0.66	38.8	2.53	968	776	955	No
11		SPSW S	2	1:1	0.66	36.5	3.01	752	675	705	No

Table 1. Evaluation of VBE Shear Demand and Strength[a]

[a] For multi-story specimens, VBEs at the first story are evaluated.
[b] Not applicable.
[c] Using the first-story height.
[d] The plastic moments applied at the VBE ends are equal to the strength of web–angle beam-to-column flexible connections.

$$V_n = 0.6f_y d_{ci} t_{wci} \qquad (10)$$

where

h_{wci} = VBE web depth
t_{wci} = VBE web thickness
E = young's modulus

It should be noted that, for simplicity here, Equation 10 does not take into account the reduction effects on the VBE shear resistance due to the presence of other internal forces in VBEs and such a simplification may lead to a VBE design that is not conservative. However, when necessary, the interaction of these effects can be considered using a more rigorous procedure provided in Qu and Bruneau (2008).

OBSERVATION OF VBE SHEAR YIELDING IN PAST TESTING

To check whether VBE shear yielding had occurred in previous tests, a selection of SPSWs for which the experimental data are available is assessed in Table 1. Those examples include both single-story and multi-story SPSWs. Using the analytical model proposed in prior section, the shear demands (i.e., $V_{u\text{-}design}$) and strengths (i.e., V_n), respectively calculated using Equations 9 and 10, are presented in Table 1. Using published information on SPSW geometries and member sizes, strip models for those considered SPSWs were devel-

oped, and the corresponding maximum VBE shears obtained from the pushover analysis using SAP2000 (i.e., $V_{pushover}$) are also provided in Table 1. Note that 20 strips were used for the infill plates at each story in all specimens. Steel was modeled as an elasto–perfectly plastic material using the yield strength provided in each relevant reference. Plastic hinges accounting for the interaction of axial force and flexure were defined at the ends of HBEs and the VBE bases. The vertical distributions of lateral forces used in the pushover analyses were determined according to the loading conditions reported for each actual test. For comparison purposes, specimen scale, aspect ratio and tension field inclination angle of those considered SPSWs are provided in Table 1.

Comparing $V_{pushover}$ to $V_{u\text{-}design}$, Table 1 confirms that Equation 9 gives conservative VBE design shear forces (as expected since it assumes plastic hinges at both ends of the VBE). The level of conservation varies from 0.7% to 57%, and is, on average, 25% for the cases considered.

On the other hand, comparing V_n to $V_{pushover}$ reveals that the VBEs in cases 1, 3, 6, 7 and 8 should have experienced shear yielding during their tests while the VBEs in other cases would not. This prediction is consistent with experimental observations. For a better understanding, the following will focus on the observed VBE behaviors in cases 1, 3, 6, 7 and 8.

For the SPSW of case 1 [i.e., the single-story SPSW (SPSW2) tested by Lubell et al. (2000)], significant inward deformations were observed in the VBEs as shown in Figure 6. Montgomery and Medhekar (2001) ascribed this undesirable VBE behavior to: (1) the small infill panel width-to-height aspect ratio compared to other specimens for which the VBEs exhibited desirable behavior, (2) relative small tension field inclination angle calculated per the equation provided in the AISC *Seismic Provisions* and CSA S16-01, and (3) excessive VBE flexibility.

The fact that the single-story specimen had a width-to-height infill panel aspect ratio of approximately 1.0, by itself, should not be a concern contrary to the claim by Montgomery and Medhekar (2001). This is because the VBEs of the MCEER/NCREE full-scale two-story SPSW specimen, which had the same width-to-height aspect ratio of 1.0, exhibited desirable VBE performance (Qu et al., 2008), and others have also tested narrow SPSWs that exhibited equally satisfactory behavior (e.g., Lee and Tsai, 2008, used an aspect ratio of 0.66).

In addition, the tension field inclination angle of the single-story specimen calculated per the AISC *Seismic Provisions* (AISC, 2005c) and CSA S16-01 is 37.4°. That, by itself, should not be a reason for the observed undesirable VBE behavior. As presented in Table 1, the two-story SPSW (specimen SPSW S) recently tested by Lee and Tsai (2008) had an even smaller inclination angle of 36.5° and exhibited satisfactory VBE performance up to story drifts greater than 5%.

As to whether the undesirable VBE inward deformation observed in the single-story specimen can be attributed to excessive VBE flexibility, even though this specimen had a flexibility factor of 3.35 (i.e., greater than the code specified limit of 2.5), the results in Table 1 demonstrate that VBE shear yielding occurred in that specimen during the tests, resulting in the significant in-plane VBE deflection due to inelastic shear deformations. Yielding pattern of the VBE webs further confirms this point. As indicated by the flaked whitewash shown in Figure 6, the VBE web yielded uniformly at the VBE ends as opposed to the yielding pattern usually observed in flexural plastic hinges, indicating significant inelastic shear deformations. Note that the axial force in the VBEs can also affect the yielding pattern of VBE webs. However, the axial force developed in the VBEs is insignificant in this single-story case.

For the SPSW of case 3 (i.e., the four-story SPSW tested by Driver et al., 1997), deformations at the first story of the wall are shown in Figure 8. Note that this specimen had a code-compliant flexibility factor of 1.73. Incidentally, plastic strength of the wall predicted using the procedure proposed by Berman and Bruneau (2003), which has been verified by numerous other experimental results, is substantially greater than the strength obtained during the test. Sabouri-Ghomi (2005) alleged that the reduced plastic strength of the wall could be due to overall bending effects. However, results shown in Table 1 unequivocally show that VBE shear yielding occurred in the first-story of that specimen. This may have resulted in incomplete development of the expected VBE plastic moments and infill tension field at the first story, and thus the lower plastic base shear compared to the predictions from plastic analysis. Interestingly, fractures were observed to penetrate into the VBE web at the column bases during tests, which may also be related to the significant shear force acting there.

Cases 6, 7 and 8 are three-story specimens from a series of tests on SPSWs by Park et al. (2007). For comparison purpose, case 6 is first compared against cases 4 and 5. Specimens of cases 4, 5 and 6 (i.e., SC2T, SC4T and SC6T, respectively, in Park et al., 2007) have flexibility factors of 1.24, 1.44 and 1.58, respectively, which all satisfied the code-specified limit of 2.5. These specimens had identical boundary frame members and constant infill panels along the height of each wall [with thicknesses of 2 mm, 4 mm and 6 mm in SC2T, SC4T and SC6T, respectively (0.08 in., 0.16 in. and 0.24 in.)]. These specimens had the same VBE members and thus the same shear strength per Equation 10. However, the shear demands on the first-story VBEs of SC2T, SC4T and SC6T increased directly as a function of the infill panel yield forces, which are determined from the infill panel thicknesses. As shown from the results in Table 1, the first-story VBEs of SC6T are expected to yield in shear while those of SC2T and SC4T would not. This prediction agrees with the observed yielding patterns shown in the photos presented in Park et al. (2007).

For the specimens in cases 7 and 8 [i.e., WC4T and WC6T in Park et al. (2007), respectively], the VBEs were wide flange members with noncompact flanges. WC4T and WC6T have code-compliant flexibility factors of 1.62 and

*Fig. 8. First story of Driver's SPSW
(photo courtesy of R.G. Driver).*

1.77, respectively. However, significant pull-in deformations were observed in the VBEs of these two specimens. Local buckling due to flange noncompactness is an important factor that contributed to the VBE deflections during these tests, but the results in Table 1 indicate that shear yielding also developed in those VBEs. The observed VBE yielding pattern and deformation further confirm this point. As shown in the photos published by Park et al. (2007), yield lines gradually developed in the VBE web with the increases of story drift, indicating the development of VBE shear yielding, which finally resulted in significant inward deflections in the VBEs.

As discussed earlier, undesirable inward VBE deflections were observed in SPSW specimens with and without code-compliant flexibility factors. There is no correlation between flexibility factor and significant VBE pull-in deformations. Based on the analytical work conducted in this section, the observed undesirable VBE deflections were mainly caused by VBE shear yielding.

VBE Out-of-Plane Buckling

Besides the aforementioned excessive pull-in deformations, another undesirable behavior of VBE is out-of-plane buckling, which has been observed during the tests on a quarter-scale four-story SPSW specimen by Lubell et al. (2000). Confusion exists at whether this undesirable performance was also ascribed to the insufficient VBE stiffness; the AISC 341-05 commentary is not clear in this regard. At the time of this writing, no theoretical work has been conducted to establish the correlation between ωt and out-of-plane buckling strength of VBEs.

This section will investigate whether the available database of test results sustain the use of flexibility limit for VBE design to successfully prevent the out-of-plane buckling of VBE, or whether different methods are necessary for that purpose. To be able to do such comparisons, analytical models to estimate the out-of-plane buckling strength of VBEs are provided based on simple free body diagrams and the energy method taking into account representative boundary conditions of VBEs. Using the proposed analytical models, the out-of-plane behaviors of VBEs in a few representative tested SPSWs that have various values of flexibility factor are reviewed.

ANALYTICAL MODELS FOR OUT-OF-PLANE BUCKLING STRENGTH OF VBES

Free Body Diagrams of VBEs

Figure 9 shows free body diagrams of the left and right VBEs in a typical single-bay multi-story SPSW when the expected plastic mechanism of the wall develops under the rightward lateral forces. In the free body diagrams, ω_{xci} and ω_{yci} represent horizontal and vertical components of the

infill plate yield force along the VBE; P_{bli} and P_{bri} represent the axial forces at the left and right ends of HBE; V_{li} and V_{ri} represent the shear forces at the left and right VBE faces; M_{li} and M_{ri} represent the moments at the left and right VBE faces; R_{xl}, R_{xr}, R_{yl}, R_{yr}, M_{cl} and M_{cr} represent the reaction forces at VBE bases; and F_i represents the applied lateral forces to develop the expected plastic mechanism. Note that the free body diagrams of Figure 9 are only for illustration purpose and the forces shown in the figure may have a different direction depending on the equilibrium of the free body.

Free body diagram of the VBE on the right-hand side is chosen for derivation of the out-of-plane buckling strength of VBE, since the compression effect in that VBE due to the HBE end shears is additive to that from the vertical component of the infill panel yield forces along that VBE. The compression at the top end of the considered VBE, P_{topi}, can be obtained as:

$$P_{topi} = \sum_{j=i}^{n_s} V_{rj} + \sum_{j=i+1}^{n_s} \omega_{ycj} \cdot h_{sj} \tag{11}$$

where n_s is the number of stories and all other terms have been defined previously.

To ensure desirable VBE behavior, it is recommended, although slightly conservative, to neglect the reduction effects on HBE plastic moment accounting for the presence of axial force, shear force, and vertical stresses in HBE when calculating V_{rj} for determination of the VBE axial forces. In addition, it is assumed that plastic hinges form at the column face when reduced beam section (RBS) connections (ANSI/AISC 358-05) are not used in HBEs. Accordingly, the right-end shears of HBEs are obtained as:
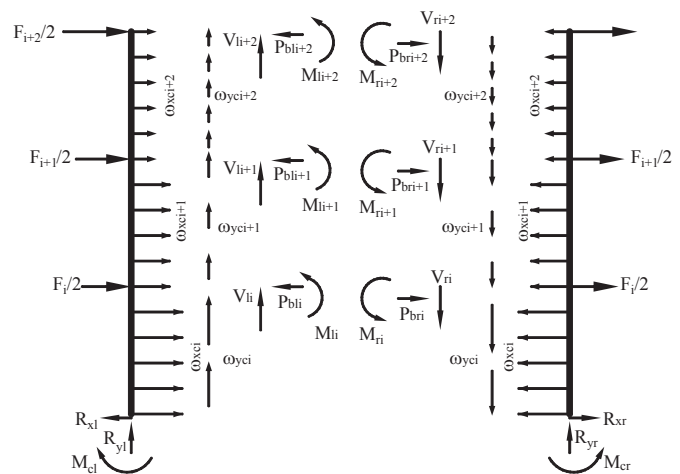

Fig. 9. VBE free body diagrams.

$$V_{ri} = \frac{\left(\omega_{ybi} - \omega_{ybi+1}\right)L}{2} + \frac{\left(\omega_{xbi} + \omega_{xbi+1}\right)d}{2} + \frac{2R_y f_y Z_{ef}}{L_h} \quad (12)$$

where

ω_{xbi} = horizontal component of the infill plate yield forces along HBE (Berman and Bruneau, 2008)

ω_{ybi} = vertical component of the infill plate yield forces along HBE (Berman and Bruneau, 2008)

d = HBE depth

L = distance between the column faces

L_h = distance between plastic hinge locations

Z_{ef} = effective plastic section modulus of HBEs

Note that Z_{ef} is equal to the plastic section modulus of a HBE when RBS connections are not used. For a HBE without RBS connections Z_{ef} should be determined according to the equations proposed by Qu and Bruneau (2008) to account for the variation of plastic hinge location in the RBS zone.

Energy Method and Boundary Conditions

Although modeling the considered VBE in some FE software packages such as ABAQUS is always possible, at the cost of computational efforts, it is relatively expedient and efficient here to illustrate important trends by using the energy method to approximately calculate the critical buckling strength of VBEs (i.e., the Euler buckling strength assuming elastic behavior and no initial imperfection in the member). It is recognized that the actual buckling strength of the member considering the previously mentioned effects would be lower and that the buckling strength calculated by this approach is optimistic. It should, therefore, not be used for design.

A rigorous derivation of the buckling strength of VBEs which takes into account inelastic behaviors and all possible boundary conditions of VBEs is complex and would be a major undertaking beyond the scope of this paper. For example, one major impediment is how to consider the boundary conditions of VBEs due to the infill panels. Note that the infill panels provide tension-only supports along the VBEs while exerting longitudinal and transverse loads along VBEs. While awaiting further research results on the buckling strength of VBEs, it is recommended to continue designing VBEs as beam-columns according to Chapter H of ANSI/AISC 360-05 for conservative combinations of maximum acting moment, shear, and axial forces, assuming conservative unsupported lengths.

However, the work presented here, even though based on elastic analysis and idealized properties, is important and included for the following reasons. First, while it is always possible to achieve conservative VBE designs (as described earlier), the objective here is to review behavior of VBEs in prior tests and attempt to see if the observed out-of-plane buckling failure can be predicted. In that perspective,

a conservative design model is of limited value. Second, if the simplified idealized elastic model considered here predicts buckling, then it is reasonably certain that the actual VBE would buckle (given that inelastic behavior and initial imperfections would reduce buckling strength). As such, a prediction of VBE buckling using the simplified approach proposed here can be helpful to confirm the case where buckling was observed in the experimental studies reviewed in this paper (recognizing that a prediction of non-buckling is not a guarantee of satisfactory performance). Finally, the results obtained using the idealized model, in spite of its own shortcomings, help bring attention to some of the important issues that must be considered in future more complex models such as boundary conditions and loads applied by the infill plate along the length of the VBEs. As such, the analytical models assuming elastic buckling behaviors of VBEs provide some of the building blocks and important perspectives necessary to derive the more advanced analytical models for calculating VBE buckling strength accounting for inelastic behavior and more complicated boundary conditions in future investigations.

The energy method considered in this paper is used in buckling problems to determine approximate values of the critical buckling strength when an exact solution of the differential equation of the deflection curve is either unknown or too complicated. In such cases, solution proceeds by assuming a reasonable shape for the deflection curve. While it is not essential for an approximate solution that the assumed curve perfectly match the deflected shape, it should satisfy the boundary conditions at the ends of the member. Using a reasonable assumed shape for the deflection curve, the energy method can give an approximate out-of-plane buckling strength of VBE, within the previously enunciated constraints (Timoshenko and Gere, 1961).

Figure 10 illustrates orientations of the VBE weak and strong axes in a typical SPSW, for which the smaller and greater moments of inertia of the VBE cross-section can be obtained. Note that VBE out-of-plane buckling develops in the plane perpendicular to the weak axis. The ends of VBEs
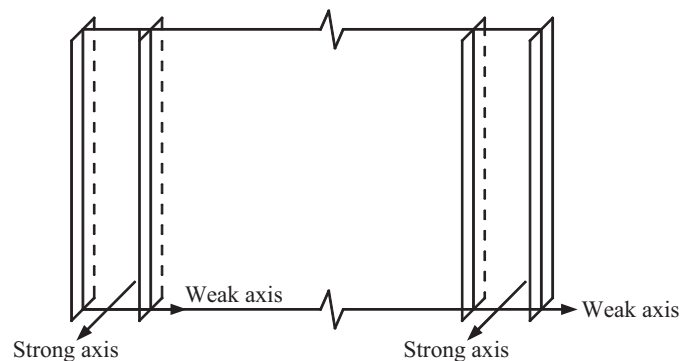

Fig. 10. Strong and weak axes of VBEs.

Factors	Case A	Case B	Case C	Case D
Shape function	$y = \delta_i \sin\left(\dfrac{\pi x}{h_{si}}\right)$	$y = \delta_i \left[1 - \cos\left(\dfrac{2\pi x}{h_{si}}\right)\right]$	$y = \delta_i \left[2x^4 + 3x^2 h_{si}^2 - 5x^3 h_{si}\right]$	$y = \delta_i \left[2x^4 - 3x^3 h_{si} + x h_{si}^3\right]$
External work	$\dfrac{\pi^4 \delta_i^2 EI_{yi}}{4h_{si}^3}\left(m + \dfrac{n}{2}\right)$	$\dfrac{\pi^4 \delta_i^2 EI_{yi}}{h_{si}^3}\left(m + \dfrac{n}{2}\right)$	$\dfrac{6\pi^2 \delta_i^2 EI_{yi} h_{si}^5}{35}\left(m + \dfrac{3n}{8}\right)$	$\dfrac{6\pi^2 \delta_i^2 EI_{yi} h_{si}^5}{35}\left(m + \dfrac{5n}{8}\right)$
Strain energy	$\dfrac{\pi^4 \delta_i^2 EI_{yi}}{4h_{si}^3}$	$\dfrac{4\pi^4 \delta_i^2 EI_{yi}}{h_{si}^3}$	$\dfrac{18\delta_i^2 EI_{yi} h_{si}^5}{5}$	$\dfrac{18\delta_i^2 EI_{yi} h_{si}^5}{5}$
Criterion	$m + \dfrac{n}{2} = 1$	$\dfrac{m}{4} + \dfrac{n}{8} = 1$	$\dfrac{\pi^2}{21}m + \dfrac{\pi^2}{56}n = 1$	$\dfrac{\pi^2}{21}m + \dfrac{5\pi^2}{168}n = 1$

[a] An arbitrarily selected nonzero deflection factor, δ_i, is used in the shape function. Note that the magnitude of δ_i has no impact on the buckling strength of VBE.

are laterally supported by the floor system, and the first-story VBE is either fixed or pinned to ground. Under those conditions, the out-of-plane translations at the VBE ends are restrained. However, the out-of-plane rotational restraints due to the beams framing into the VBEs can vary from fully free to fully fixed and would have to be assessed on a case by case basis. The VBE end conditions considered in this paper are illustrated in Figure 11(a) and correspond to ideal cases.

Criteria for the Considered Boundary Conditions

The out-of-plane buckling strength of VBE under each case of boundary conditions can be obtained following the classic procedure of energy method and the detailed derivations are presented in Qu and Bruneau (2008). In such derivation, the internal strain energy is obtained by accounting for the curvature determined from the assumed VBE deflection curve, and the external work is obtained by combining the contribution due to the concentrated force applied at the top of the VBE and that due to the infill panel yield forces along the VBE. Setting the internal strain energy equal to the external work, one can obtain the criterion to calculate the out-of-plane buckling strength of VBE. Deflection curve, internal strain energy, external work, and criterion of each considered case are presented in Table 2.

For each case of boundary conditions, the corresponding criterion that defines the buckling limit state can be expressed as a combination of m and n equal to unity, where m and n are the generalized external forces and can be respectively obtained by normalizing the concentrated force applied at the top of the VBE (i.e., P_{topi}) and the resultant infill panel yield force along the VBE (i.e., $\omega_{yci} h_{si}$), by the Euler buckling load of a simply supported VBE without any intermediate loads along its height. Namely, m and n can be determined as:

$$m = \frac{P_{topi}}{\left[\dfrac{\pi^2 EI_{yi}}{h_{si}^2}\right]} \quad \text{and} \quad n = \frac{\omega_{yci} h_{si}}{\left[\dfrac{\pi^2 EI_{yi}}{h_{si}^2}\right]} \tag{13}$$

where I_{yi} is the moment of inertia of the VBE taken from the weak axis.

Graphical versions of the criteria presented in Table 2 are shown in Figure 11(b). For a given load combination (i.e., a pair of m and n) and boundary conditions, if the left-hand side of the corresponding criterion presented in Table 2 is greater than 1, the VBE is expected to encounter out-of-plane buckling. Those combinations for which buckling failure occurs are represented by the shaded area in Figure 11(b). Incidentally, using an alternative approach based on the differential equations of beam-column theory, Timoshenko and Gere (1961) provided the critical buckling strength of the column under Case A boundary conditions for a few selected individual scenarios. Their results are also presented in Figure 11(b). As expected, a good agreement is observed. As shown, for each case, the value of m decreases when the value of n increases, which physically means that lower concentrated force needs to be applied at the top of the column to avoid column buckling when higher infill panel yield forces are applied. Note that parts of Figure 11 are presented with different vertical axes to purposely improve legibility. It also should be mentioned that the negative range of m in Criterion A is reasonable and it is consistent with the fact that, when large infill panel yield forces are applied along the column (which corresponds to large values of n), the axial force required at the top end of the member to avoid out-of-plane buckling failure should be upward (i.e., it should be a tensile force which corresponds to the negative value of m).

REVIEW OF OUT-OF-PLANE BUCKLING
OF VBES IN PAST TESTS

To better understand the VBE out-of-plane buckling behavior, performance of the VBEs in previously tested SPSWs are revisited in perspective of the criteria derived in the previous section to see whether the proposed alternative approach can shed additional light on the behavior of VBEs.
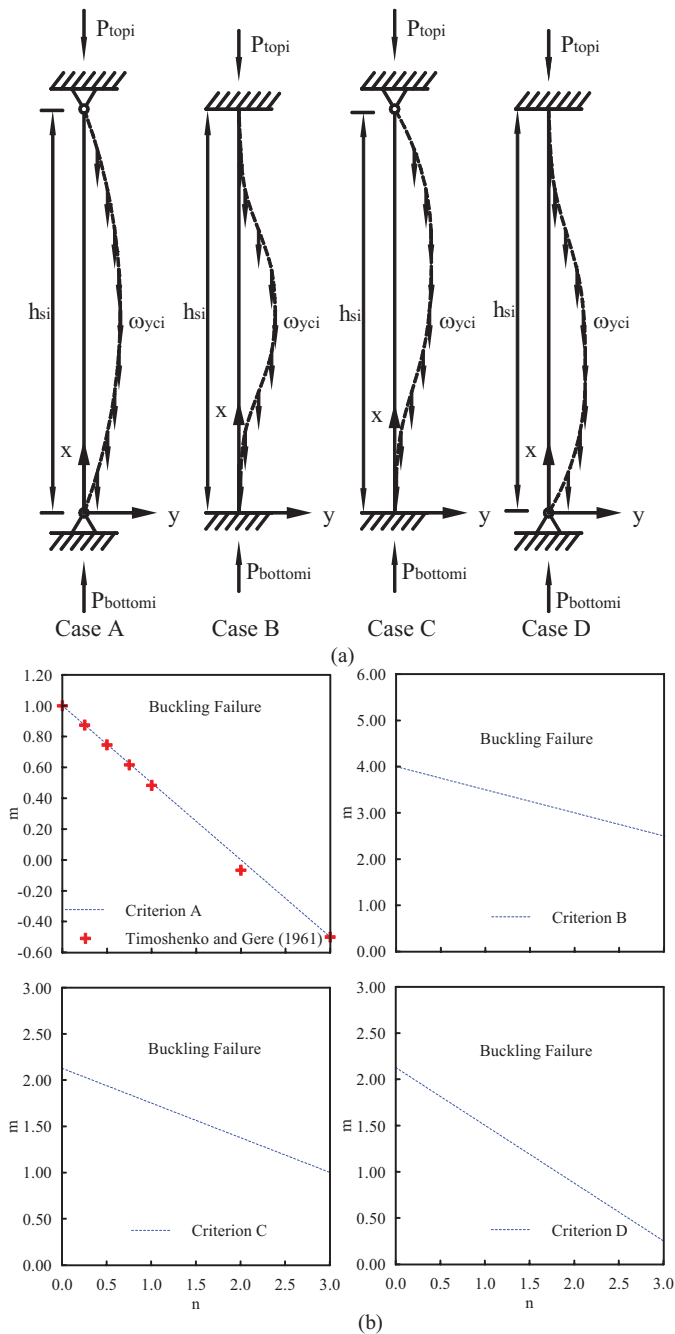

Fig. 11. Out-of-plane buckling of VBE: (a) considered boundary conditions; (b) interaction of critical loads.

The considered SPSW specimens are assessed using the criteria developed for the four boundary conditions considered since the out-of-plane restraints at the ends of the VBEs of some specimens are not provided in the available references. As shown by the results presented in Table 3, no matter what boundary conditions were applied, VBE out-of-plane buckling would not be predicted to occur in any of the SPSWs except for the Lubell et al. (2000) quarter-scale four-story SPSW. This prediction is consistent with the observations on those SPSWs obtained during tests, validating to some degree the proposed analytical models for calculating VBE out-of-plane buckling strength. Note that for this Lubell et al. specimen insignificant amounts of hysteretic energy were dissipated before instability of VBE precipitated the system failure.

A closer look at the Lubell et al. specimen and the buckled shape of its VBE reveals that Case C boundary conditions were present (i.e., bottom end of the VBE was fixed to the ground while the top end was pinned in the out-of-plane direction). To better understand this, the VBE deflection traced from the specimen is superposed to those corresponding to cases B and C boundary conditions in Figure 12. Comparing the deflected shapes confirms that the VBE end conditions correspond to those of Case C. Accordingly, applying Criterion C provides a value of 1.066 greater than 1.0 as shown in Table 3, indicating the expected occurrence of VBE out-of-plane buckling. This suggests that out-of-plane buckling of the VBEs in the Lubell et al. specimen can be rationally predicted using the out-of-plane buckling equations derived here rather than excessive VBE flexibility.

Two other interesting cases in Table 3 are the two specimens (i.e., SPSW N and SPSW S) tested by Lee and Tsai (2008). SPSW N and SPSW S, respectively, had flexibility factors of 2.53 and 3.01 (i.e., above the code-specified upper
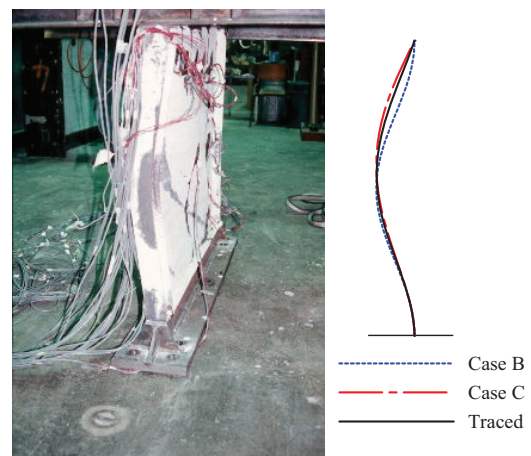

Fig. 12. Out-of-plane buckling of bottom VBE
(photo courtesy of C.E. Ventura).

Table 3. Evaluation of VBE Out-of-Plane Buckling[a]

Case	Researcher	Specimen Identification	Number of Stories	ω_t	Criterion A	Criterion B	Criterion C	Criterion D
(i) single-story specimens								
1	Lubell et al. (2000)	SPSW2	1	3.35	0.609	0.152	0.260	0.313
2	Berman and Bruneau (2005)	F2	1	1.01	0.006	0.001	0.002	0.003
(ii) multi-story specimens								
3	Driver et al. (1998)	[b]	4	1.73	0.159	0.040	0.073	0.077
4	Lubell et al. (2000)	SPSW4	4	3.35	2.325	0.581	1.066	1.119
5	Park et al. (2007)	SC2T	3	1.24	0.051	0.013	0.024	0.024
6		SC4T	3	1.44	0.087	0.022	0.040	0.042
7		SC6T	3	1.58	0.115	0.029	0.053	0.055
8		WC4T	3	1.62	0.142	0.036	0.065	0.068
9		WC6T	3	1.77	0.188	0.047	0.086	0.090
10	Qu et al (2008)	[b]	2	1.95	0.238	0.060	0.107	0.116
11	Lee and Tsai (2007)	SPSW N	2	2.53	0.111	0.028	0.050	0.054
12		SPSW S	2	3.01	0.199	0.050	0.090	0.097

[a] For multi-story specimens, VBEs at the first story are evaluated.
[b] Not applicable.

limit of 2.5). Yet, based on the proposed analytical models, the VBEs in these two specimens are not expected to undergo out-of-plane buckling. This prediction is consistent with the experimental observations. The VBEs of these two specimens exhibited ductile behavior up to story drifts greater than 5%. The assessment on SPSW N and SPSW S further confirms that there is no correlation between the flexibility factor, ω_t, and VBE out-of-plane buckling strength.

CONCLUSIONS

In this paper, analytical work was conducted to assess the adequacy of the existing limit on the flexibility factor, ω_t, specified for VBE design by the AISC *Seismic Provisions* and CSA S16-01. Review of the derivations of this flexibility factor from plate girder theory and how that factor was incorporated into current design codes was followed by the development of analytical models for preventing VBE shear yielding and for estimating out-of-plane buckling strength of VBEs in SPSWs.

It is shown that the existing limit on ω_t is uncorrelated to satisfactory in-plane and out-of-plane VBE performance. Alternatively, the proposed analytical model for in-plane VBE shear demands, from which predicted performance correlates well with past experimental results, can be used to ensure desirable VBE behavior. Future analytical and experimental research should investigate whether in-plane buckling

equations similar to those used for out-of-plane buckling are necessary for use in the interaction equations to calculate the beam-column strength of VBEs, and whether other concerns may justify retaining the use of ω_t factor to achieve satisfactory seismic performance of VBEs in SPSWs.

REFERENCES

AISC (2005a), ANSI/AISC 358-05, *Prequalified Connections for Special and Intermediate Steel Moment Frames for Seismic Applications*, American Institute of Steel Construction, Chicago, IL.

AISC (2005b), ANSI/AISC 360-05, *Specification for Structural Steel Buildings*, American Institute of Steel Construction, Chicago, IL.

AISC (2005c), ANSI/AISC 341-05, *Seismic Provisions for Structural Steel Buildings,* American Institute of Steel Construction, Chicago, IL.

Berman, J.W. and Bruneau, M. (2003), "Plastic Analysis and Design of Steel Plate Shear Walls," ASCE, *Journal of Structural Engineering*, Vol. 129, No. 11.

Berman, J.W. and Bruneau, M. (2004), "Steel Plate Shear Walls are Not Plate Girders," AISC, *Engineering Journal* Vol. 41, No. 3.

Berman, J.W. and Bruneau, M. (2005), "Experimental Investigation of Light-Gauge Steel Plate Shear Walls," ASCE, *Journal of Structural Engineering*, Vol. 131, No. 2.

Berman, J.W. and Bruneau, M. (2008), "Capacity Design of Vertical Boundary Elements in Steel Plate Shear Walls," AISC, *Engineering Journal,* Vol. 45, No. 1.

CSA (1994), "Limit States Design of Steel Structures," CAN/CSA S16-94, Toronto, ON, Canada.

CSA (2001), "Limit States Design of Steel Structures," CAN/CSA S16-01, Toronto, ON, Canada.

Driver, R.G., Kulak, G.L., Kennedy, D.J.L. and Elwi, A.E. (1998), "Cyclic Test of a Four-Story Steel Plate Shear Wall," ASCE, *Journal of Structural Engineering*, Vol. 124, No. 2.

FEMA (2003), "NEHRP Recommended Provisions for Seismic Regulations for New Buildings and Other Structures," FEMA 450, prepared by the Building Seismic Safety Council for FEMA, Washington, D.C.

Lee, C.S. and Tsai, K.C. (2008), "Experimental Response of Four 2-Story Narrow Steel Plate Shear Walls," *Proceedings of the 2008 Structures Congress*, Vancouver, BC, Canada.

Lubell, A.S., Prion, H.G.L., Ventura, C.E. and Rezai, M. (2000), "Unstiffened Steel Plate Shear Wall Performance under Cyclic Loading," ASCE, *Journal of Structural Engineering*, Vol. 126 No. 4.

Kuhn, P., Peterson, J.P. and Levin, L.R. (1952), "A Summary of Diagonal Tension. Part I: Methods and Analysis," Technical Note 2661, National Advisory Committee for Aeronautics, Washington, D.C.

Montgomery, C.J. and Medhekar, M. (2001), "Discussion on Unstiffened Steel Plate Shear Wall Performance under Cyclic Loading," ASCE, *Journal of Structural Engineering*, Vol. 127, No. 8.

Park, H.G., Kwack, J.H., Jeon, S.W., Kim, W.K. and Choi, I.R. (2007), "Framed Steel Plate Wall Behavior under Cyclic Lateral Loading," ASCE, *Journal of Structural Engineering*, Vol. 133, No. 3.

Qu, B., Bruneau. M., Lin, C.H. and Tsai, K.C. (2008), "Testing of Full Scale Two-story Steel Plate Shear Walls with RBS Connections and Composite Floor," ASCE, *Journal of Structural Engineering*, Vol. 134, No. 3.

Qu, B. and Bruneau. M. (2008), "Seismic Behavior and Design of Boundary Frame Members of Steel Plate Shear Walls," Technical Report MCEER-08-0012, Multidisciplinary Center for Earthquake Engineering Research, Buffalo, NY.

Sabelli, R. and Bruneau, M. (2007), *AISC Design Guide 20, Steel Plate Shear Walls,* American Institute of Steel Construction, Chicago, IL.

Sabouri-Ghomi, S. (2005), "Discussion of Plastic Analysis and Design of Steel Plate Shear Walls," ASCE, *Journal of Structural Engineering*, Vol. 131, No. 4.

Timoshenko, S.P. and Gere, J.M. (1961), *Theory of Elastic Stability*, 2nd edition, McGraw-Hill Book Company, Inc., New York, NY.

Vian, D. and Bruneau M. (2005), "Steel Plate Shear Walls for Seismic Design and Retrofit of Building Structure," Technical Report MCEER-05-0010, Multidisciplinary Center for Earthquake Engineering Research, Buffalo, NY.

Wagner, H. (1931), "Flat Sheet Metal Girders with Very Thin Webs, Part III: Sheet Metal Girders with Spars Resistant to Bending—The Stress in Uprights—Diagonal Tension Fields," Technical Memorandum No. 606, National Advisory Committee for Aeronautics, Washington, D.C.